Crystallization of D-Mannitol in Binary Mixtures with NaCl: Phase Diagram and Polymorphism

Chitra Telang,[1] Raj Suryanarayanan,[1] and Lian Yu[2,3,4]

Received May 23, 2003; accepted August 6, 2003

Purpose. To study the crystallization, polymorphism, and phase behavior of D-mannitol in binary mixtures with NaCl to better understand their interactions in frozen aqueous solutions.

Methods. Differential scanning calorimetry, hot-stage microscopy, Raman microscopy, and variable-temperature X-ray diffractometry were used to characterize D-mannitol–NaCl mixtures.

Results. NaCl and D-mannitol exhibited significant melt miscibility (up to 7.5% w/w or 0.20 mole fraction of NaCl) and a eutectic phase diagram (eutectic composition 7.5% w/w NaCl; eutectic temperature 150°C for the α and β polymorphs of D-mannitol and 139°C for the δ). The presence of NaCl did not prevent mannitol from crystallizing but, depending on sample size, affected the polymorph crystallized: below 10 mg, δ was obtained; above 100 mg, α was obtained. Pure mannitol crystallized under the same conditions first as the δ polymorph and then as the α polymorph, with the latter nucleating on the former. KCl showed similar eutectic points and melt miscibility with D-mannitol as NaCl. LiCl yielded lower eutectic melting points, inhibited the crystallization of D-mannitol during cooling, and enabled the observation of its glass transition.

Conclusions. Despite their structural dissimilarity, significant melt miscibility exists between D-mannitol and NaCl. Their phase diagram has been determined and features polymorph-dependent eutectic points. NaCl influences the polymorphic behavior of mannitol, and the effect is linked to the crystallization of mannitol in two polymorphic stages.

KEY WORDS: D-mannitol; NaCl; eutectic; polymorph; phase diagram.

INTRODUCTION

A previous study from our laboratories showed that NaCl effectively inhibits the crystallization of D-mannitol in frozen aqueous solutions, outperforming polyvinylpyrrolidone, polyethylene glycol, polysorbate, poloxamer, and alditols (1). For example, alditols [$HOCH_2(CHOH)_nCH_2OH$], the most effective non-salt inhibitors tested, prevented mannitol crystallization during cooling at a 1**:**1 alditol:mannitol ratio, but NaCl was effective at 0.1**:**1 NaCl:mannitol ratio. To better understand this phenomenon, the present study investigated how D-mannitol and NaCl, two structurally dissimilar solutes frequently used in lyophilization, interact in binary mixtures.

Understanding solute–solute interactions is pertinent to the design of freeze-drying protocols. Once ice crystallizes, the concentrated solutes may crystallize or remain amorphous (2,3). Sucrose, for example, generally remains amorphous and can inhibit the crystallization of other solutes (4,5). Phase and state diagrams are effective tools for describing the interactions between components and for selecting excipients and their optimal concentrations (2,6,7).

D-Mannitol (hereafter abbreviated as mannitol) is a versatile excipient whose physical state can be engineered to meet the diverse requirements of formulation development. When used as a bulking agent, mannitol is frequently induced to crystallize (e.g., by annealing) (8,9). When used as a stabilizer for the active pharmaceutical ingredient (API), mannitol must be retained amorphous (10,11). To effectively control the physical state of mannitol, it is necessary to understand how other solutes affect its crystallization, both in the presence and absence of water. Although previous studies have characterized the phase behavior of aqueous solutions of mannitol (4,12), NaCl (6), and their combination (1,13), binary mixtures of mannitol and NaCl have not been studied. This study investigated how NaCl affects the crystallization of mannitol in binary mixtures to better understand the phase behavior of their aqueous solutions.

This study was also motivated by a general need to better understand the interactions between electrolyte and nonelectrolyte components in pharmaceutical formulations. Interactions between nonelectrolytes of like structures are readily visualized and predicted. For example, the sorbitol–mannitol system has been characterized (14,15) and used to extrapolate the glass transition temperature of mannitol, a property difficult to measure because of its strong tendency to crystallize (16). Relatively little attention, however, has been paid to electrolyte–nonelectrolyte interactions and the ensuing effect on the physical states of freeze-dried solutes. This study demonstrated that despite their dissimilar structures, NaCl and mannitol have significant melt miscibility, and NaCl influences the polymorphism of mannitol.

EXPERIMENTAL

Materials

D-Mannitol (99+%, Sigma-Aldrich, MO) and salts (NaCl, KCl, K_2SO_4, and LiCl; all 99+%, Fisher, NJ) were used as received. To ensure uniform mixing, mixtures of mannitol and NaCl were prepared by dissolving the components in a minimum amount of water (e.g., 20 mg of NaCl and 180 mg of mannitol dissolved in 3 ml of water) and drying at 80°C in vacuum (25 mTorr). In the first step (dissolution), water was slowly added to NaCl and mannitol until a visually clear solution was obtained. The dryness of the mixtures was ensured through thermogravimetric analysis (weight loss < 0.5% at 100°C).

Thermogravimetric analysis (TGA) was performed at 10°C/min under nitrogen purge in open Al pans using a TA SDT unit (TA Instruments, DE). The balance was calibrated against manufacture-supplied standard weights and verified against the dehydration of sodium tartrate.

Differential scanning calorimetry (DSC) was performed in crimped (non–hermetically sealed) Al pans with a TA 2920 (TA Instruments, DE) equipped with a refrigerated cooling system. Indium melting (m.p. 156.8°C and the enthalpy of fusion 3.28 kJ/mol) was used to calibrate the temperature and

[1] College of Pharmacy, University of Minnesota, Minneapolis, MN 55455.

[2] Lilly Research Laboratories, Eli Lilly and Company, Indianapolis, IN 46285.

[3] Current address: School of Pharmacy, University of Wisconsin-Madison, 777 Highland Avenue, Madison, WI 53705.

[4] To whom correspondence should be addressed. (email: lyu@pharmacy.wisc.edu)

0724-8741/03/1200-1939/0

heat flow. In a typical analysis, the sample (*ca.* 5 mg) was heated at 5°C/min to 200°C, held for 20 min, cooled at 5°C/min to –30°C, and reheated at 5°C/min to 200°C. To determine the eutectic phase diagram, a lower heating rate of 1°C/min was used. Other experimental conditions are detailed in Results and Discussion.

Hot stage microscopy (HSM) was performed with a Linkam THMS 600 hot stage and a Nikon Optiphot Pol 2 microscope. About 2 mg of a sample was heated at 10°C/min to 180°C, held for 5 min, cooled at 10°C/min to 65–70°C, and reheated at 5°C/min to 180°C.

Raman microscopy was performed with a Renishaw System 1000 micro-Raman Spectrometer. The excitation source was a 17-mW HeNe laser (633 nm). Raman scattered signal was dispersed with a 1200 lines/mm grating, providing a spectral resolution of 2 cm^{-1}, and detected by a deep depletion CCD detector with Peltier cooling (–7°C). Wavelength calibration was performed against Ne emission lines and checked daily against the Raman spectra of single-crystal silicon or cyclohexane. Raman spectra were recorded through a 50× objective from an illuminated area of *ca.* 1 μm diameter. Polymorph assignment was made in reference to the spectra of authentic mannitol polymorphs certified by XRD.

X-ray diffractometry (XRD) was performed with a Scintag Model XDS 2000 diffractometer with a variable temperature stage (Micristar, Model 828D; working temperature range of –190 to 300°C). Samples were placed on a copper sample holder. Specific experimental details are provided in Results and Discussion. XRD patterns were obtained with CuKα radiation (45 kV × 40 mA) at a scanning speed of 5°(2θ)/min and a step size of 0.03°(2θ). During each scan, the sample was maintained at a constant temperature.

RESULTS AND DISCUSSION

To systematically study the phase behavior of the mannitol–NaCl system, we first characterized a mixture containing 10% NaCl w/w and then analyzed mixtures of different compositions. The first part investigated how NaCl affected the melting, crystallization, and polymorphism of mannitol, and the second part determined the binary phase diagram of mannitol and NaCl. We also compared NaCl with other salts in their ability to influence the crystallization and polymorphism of mannitol.

Mannitol-NaCl Mixture Containing 10% NaCl w/w

XRD analysis showed that the 10% NaCl w/w mixture produced by dissolution and drying (see Experimental) contained crystalline mannitol and NaCl (Fig. 1c), with mannitol existing as a mixture of the α polymorph (major component) and the β polymorph (minor component) (17). The purchased mannitol (Fig. 1a), in comparison, was of the β polymorph. Without NaCl, the same dissolution/drying procedure yielded the α polymorph (Fig. 1b).

When the 10% NaCl w/w mixture was heated on the microscope hot stage, melting was observed at 150°C significantly below the melting points of the constituent mannitol polymorphs (165.0°C for α and 165.5°C for β, Ref. 18). By 160°C, all crystals of mannitol melted, but cubic crystals of NaCl remained up to 200°C (the final temperature of heating). On cooling, the sample recrystallized at 115°C into

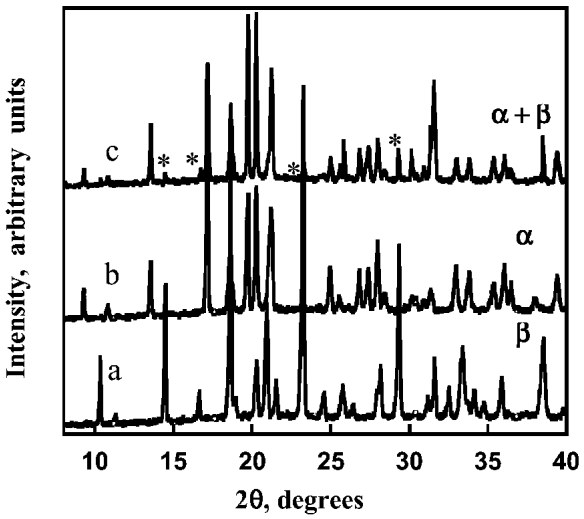

Fig. 1. X-ray diffraction data of (a) mannitol as purchased (β polymorph), (b) mannitol produced by dissolution in water and vacuum drying (α polymorph), and (c) mannitol–NaCl mixture (10% NaCl w/w) produced by dissolution in water and vacuum drying (mainly α polymorph with trace amount of β). Peaks unique to the β form have been marked with *. A peak caused by NaCl is seen at 31.6°2θ in curve c.

spherulites that were characteristically "speckled" (Fig. 2a). Raman microscopy showed that the spherulites comprised the δ polymorph of mannitol. On reheating, melting occurred at 139°C, followed immediately by recrystallization. The resulting crystals had different morphologies (Fig. 2b) and were determined by Raman microscopy to be the α polymorph (Fig. 2d). The melting temperature of 139°C was significantly below that of the δ polymorph (155°C). The "speckled" spherulites likely resulted from the crystallization of NaCl while mannitol crystallized from the melt.

DSC showed that the 10% NaCl w/w mixture melted at 150°C (Fig. 3b). On cooling the melt, a sharp crystallization exotherm occurred at 112°C (not shown). On second heating (Fig. 3c), a melting endotherm occurred at 139°C, which was followed by a crystallization exotherm and another melting endotherm at 150°C.

VTXRD was performed with a sample size (*ca.* 10 mg) comparable to that used in the DSC (Fig. 3, lower panel). When the sample was melted by heating to 200°C and cooled to 25°C, the δ polymorph crystallized (curve i). On reheating, the δ polymorph persisted up to 130°C (curve ii). At 140°C, peaks unique to the δ polymorph (e.g., at 2θ = 9.6°) disappeared, and peaks characteristic of the α polymorph appeared (curve iii). No further changes in the XRD pattern occurred up to 145°C (curve iv). At 160°C, all mannitol peaks disappeared, but peaks unique to NaCl remained.

Collectively, the results of hot stage microscopy, Raman microscopy, DSC, and VTXRD establish that in the presence of NaCl, the polymorphs of mannitol melted at approximately 15°C below the respective melting points. These results also reveal that mannitol crystallized as the δ polymorph in the presence of NaCl in the HSM, DSC, and VTXRD experiments.

The last observation deserves some attention because of the difficulty of obtaining the pure δ polymorph in large quantities. Between room temperature and its melting point, the δ

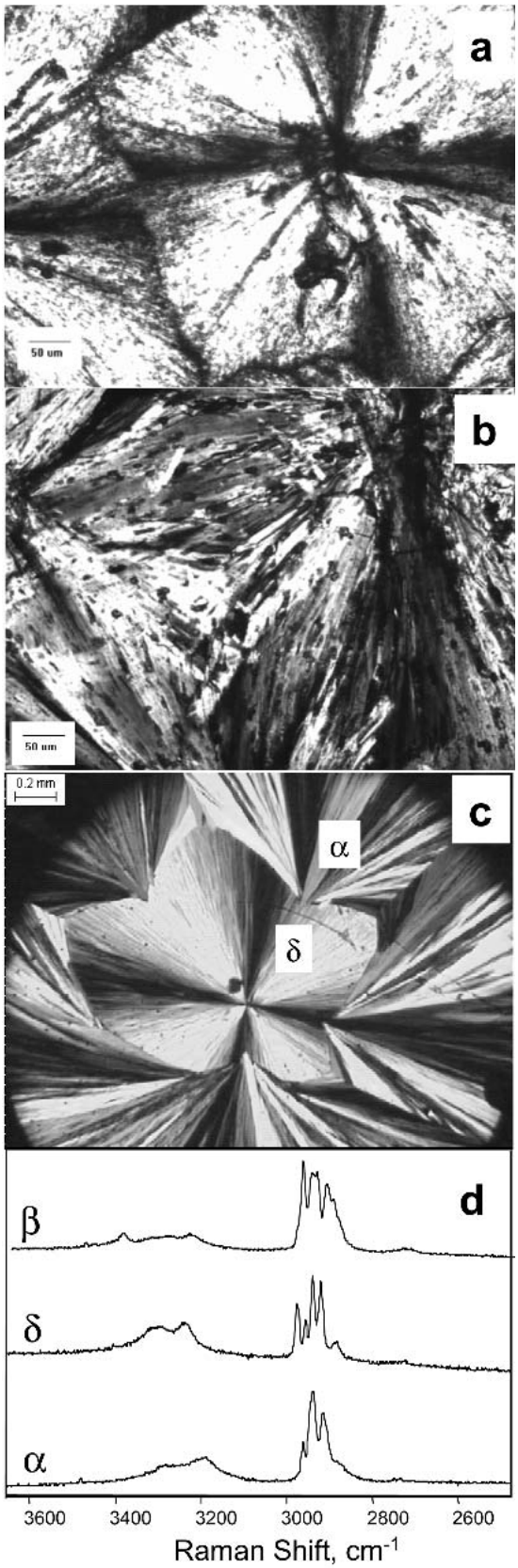

Fig. 2. (a) Spherulites of the δ polymorph of mannitol obtained after cooling a melt of the mannitol–NaCl mixture (10% w/w NaCl) from 200°C at 10°C/min. (b) The α polymorph formed after heating the sample in (a) to 145°C. (c) Same as (a), but the sample was pure mannitol. (d) Raman spectra of the polymorphs of mannitol obtained on the hot stage.

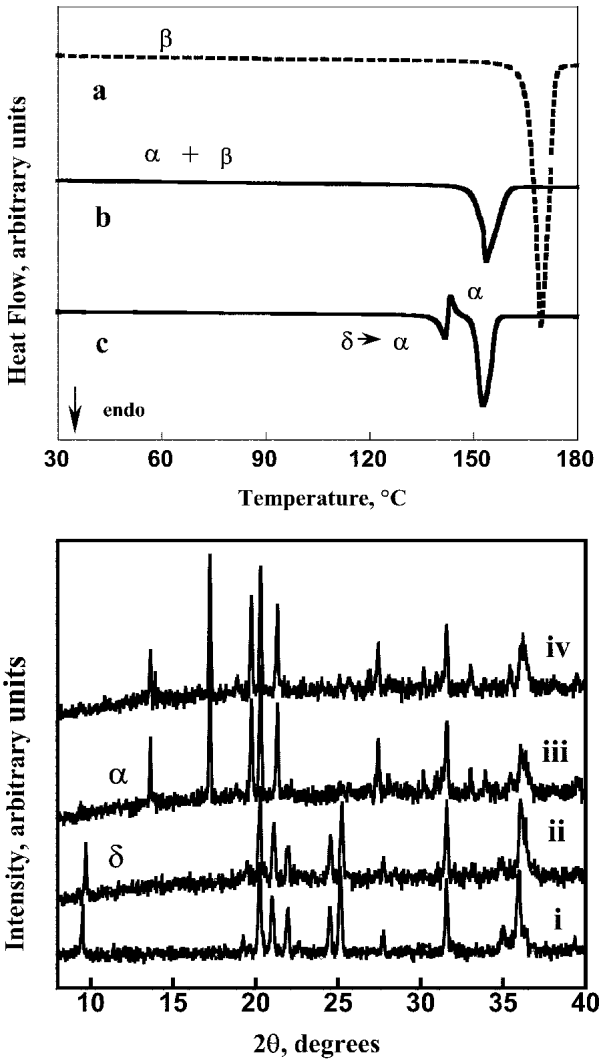

Fig. 3. Differential scanning calorimetry (top) and X-ray diffraction (XRD; bottom) data acquired on heating a mannitol–NaCl mixture (10% w/w NaCl). Top panel: (a) Melting of pure mannitol (β polymorph); (b) eutectic melting of mannitol (α and β polymorphs) with NaCl; (c) second heating after (b), showing eutectic melting of mannitol (δ polymorph) with NaCl, recrystallization to the α polymorph, and its eutectic melting. Bottom panel: XRD patterns obtained after a melt (produced by heating to 200°C) was cooled 5°C/min to 25°C and reheated 1°C/min to 25°C (i), 130°C (ii), 140°C (iii), and 145°C (iv). The NaCl peak (31.6°2θ) persists.

polymorph is metastable to the α and β polymorphs (18). Burger *et al.* suggest that the δ polymorph is enantiotropically related to the α and β polymorphs, with the transition temperatures lying below room temperature (18). Whereas the α and β polymorphs are readily crystallized from water and ethanol-water mixtures, respectively, the δ polymorph has been more difficult to produce (18,19). Once harvested from solution, crystals of the δ polymorph must be immediately filtered and dried to prevent polymorphic conversion. Low temperatures seem to favor the δ polymorph, as it frequently occurs in freeze-dried materials (18).

When pure mannitol was melted and cooled (in the same way as the 10% NaCl w/w mixture), crystallization occurred at *ca.* 120°C. XRD showed that within the limit of detection,

the product was the α polymorph; however, careful examination by HSM and Raman microscopy revealed that mannitol frequently crystallized in two stages: first as the δ polymorph and then as the α polymorph, with the latter nucleating on the former (Fig. 2c). As a result, the δ polymorph was frequently found at the centers of the spherulites of the α polymorph. This and related results have been examined elsewhere and led to the surprising conclusion that seeds of one polymorph can nucleate another (20).

The different crystallization products obtained in the presence and absence of NaCl demonstrate that NaCl influenced the polymorphic outcome and aided the isolation of the metastable δ polymorph. Because of the two-stage mechanism of mannitol crystallization (Fig. 2c), the effect of NaCl on the polymorphic outcome may stem from retarded nucleation of the α polymorph, inhibition of the δ→α transformation, or both.

To take advantage of the effect of NaCl on polymorphic outcome to produce larger quantities of the δ polymorph, we scaled up the sample size of the VTXRD experiment from 10 mg to 100 mg. At the increased sample size, however, the δ polymorph was not consistently obtained. Only one in three attempts yielded the δ polymorph, and the other two gave the α polymorph. We interpret this finding also as a result of the two-stage crystallization of mannitol. Once nucleated, the α polymorph will grow to consume the remaining liquid; hence, increasing the sample size should increase the time of crystallization and in turn the likelihood of nucleating the α polymorph and increasing its abundance in the product.

Binary Phase Diagram

To construct the binary phase diagram, we analyzed different NaCl and mannitol mixtures by DSC (Fig. 4). These mixtures were prepared by the dissolution/drying procedure described in Experimental and contained the α polymorph (major component) and the β polymorph (minor component). All the samples showed an endotherm with onset at 150°C; several samples also showed another endotherm at higher temperature. Above 8% w/w NaCl, only the 150°C melting endotherm appeared, without the higher-melting endotherm even up to 240°C (the upper limit of temperature scan that corresponded to the onset of decomposition of mannitol according to TGA). These data are consistent with a eutectic phase diagram (Fig. 5), with the first endotherm corresponding to eutectic melting and the second to the liquidus line (the depressed melting of mannitol in the presence of NaCl). The eutectic temperature is 150°C and the eutectic composition is approximately 7.5% w/w NaCl (0.20 mole fraction in NaCl). Although the sample comprised the α and β polymorphs (Fig. 1c), their eutectic melting endotherms were not resolved, which resulted from the small melting-point difference (0.5°C) between these polymorphs (18). Thus, we assign 150°C as the eutectic melting point of both the α and β polymorphs with NaCl. The appearance of only the eutectic melting endotherm at high NaCl concentration indicates that the solubility of NaCl in mannitol does not change significantly with temperature. In other words, its liquidus line is likely to be nearly vertical near the eutectic point. This is not surprising given the large difference in melting point between the two components (800 vs. 166°C).

Additional experiments were performed to confirm the eutectic composition. When mixtures containing 7 and 7.5% w/w NaCl were heated at 1°C/min, a shoulder on the low-temperature edge of the eutectic endotherm was observed. This shoulder was not resolved even at a slower heating rate of 0.1°C/min. The unresolved thermal events corresponded to the eutectic melting and the melting (dissolution) of mannitol. To resolve these events, the sample was held at 151°C, just above the eutectic temperature, for 1 h to ensure complete eutectic melting. It was then cooled to 147°C. On reheating, the eutectic melting peak was not present, indicating no eutectic recrystallization on cooling, and the mannitol melting could be better discerned (Fig. 6). At low NaCl concentra-

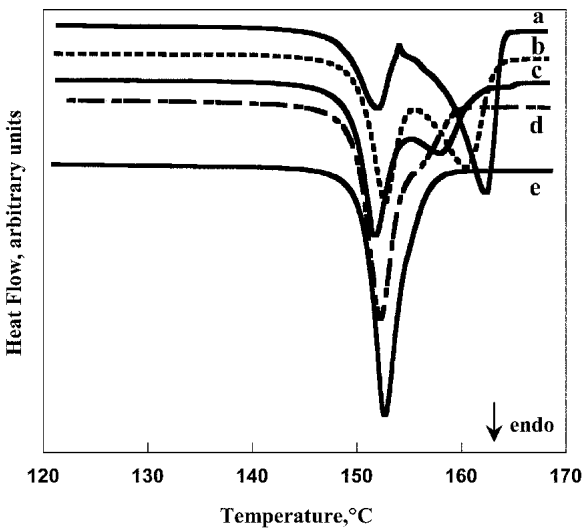

Fig. 4. Differential scanning calorimetry heating curves (1°C/min) of different mixtures of mannitol and NaCl. The NaCl concentration (% w/w) in the mixture was (a) 2, (b) 3, (c) 4, (d) 5, and (e) 7. Above 8% w/w NaCl, only the eutectic melting endotherm was observed.

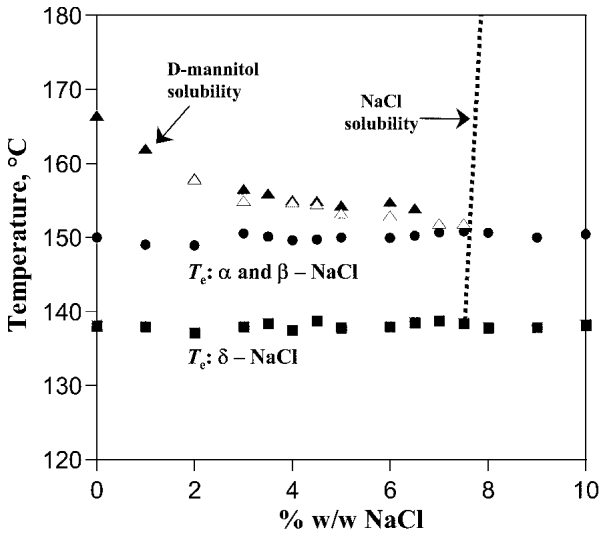

Fig. 5. Phase diagram of NaCl–mannitol. T_e is the eutectic temperature. The liquidus line of D-mannitol (the α and β polymorphs) was determined by both scanning (▲) and isothermal (△) experiments (Fig. 6). The T_es of the polymorphs of D-mannitol are distinguished by symbols: (●) for α and β and (■) for δ. The eutectic composition is 7.5% w/w NaCl. The hypothetical NaCl solubility line is nearly vertical in this temperature range because its solubility does not depend strongly on temperature.

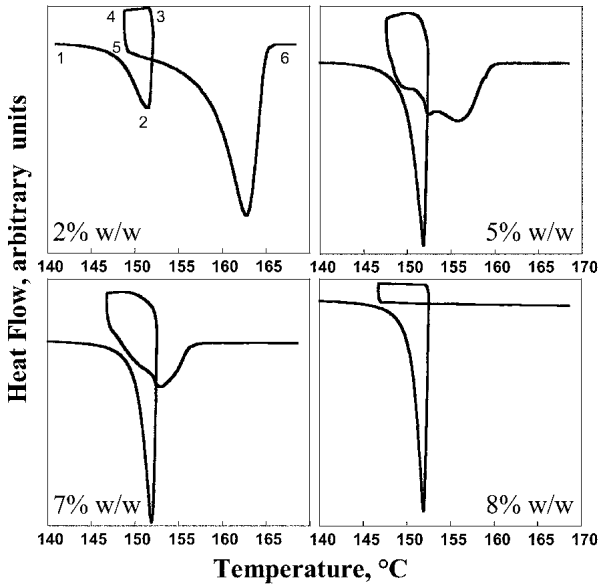

Fig. 6. Isothermal differential scanning calorimetry experiments to obtain the eutectic composition. Samples were heated to 151°C (1 to 2), held for an hour 9(2 to 3), cooled to 147°C (3 to 4), and reheated (5 to 6). The scanning rate was 1°C/min. Data are shown for four NaCl concentrations.

tions where sufficient resolution existed, the mannitol melting points determined by DSC, with and without isothermal hold, were identical. At concentrations close to 7% w/w, however, differences were evident between the mannitol melting points from the two methods. The two sets of measurement are distinguished in the phase diagram (Fig. 5). At 8% w/w, the reheating curve showed no further melting, thus confirming that the eutectic composition was below 8% w/w. The presence of crystalline NaCl was evident from its characteristic peak in the XRD pattern at 31.6°(2θ). When this peak was monitored at different concentrations around the eutectic, VTXRD results showed that the 7% w/w NaCl mixture (below the eutectic composition) fully melted at 160°C leaving no crystalline NaCl. Above 8% w/w NaCl, however, the NaCl peak persisted up to 230°C and showed no decrease in intensity with temperature (data not shown). These results indicate that the eutectic composition of NaCl and mannitol (the α and β polymorphs) is approximately 7.5% w/w NaCl.

When mannitol–NaCl mixtures were melted and cooled, the δ polymorph of mannitol crystallized from the melt. Reheating in the DSC (Fig. 3c) revealed the eutectic temperature of NaCl and the δ polymorph. The resulting data yielded the lower horizontal line in Fig. 5 at 139°C. The δ polymorph immediately converted to the α after melting, which precluded the determination of the liquidus phase boundary of the δ polymorph and the eutectic composition in the manner illustrated in Fig. 4. Despite this difficulty, the steepness of the NaCl liquidus line implies that the eutectic composition of the δ polymorph is close to that of the α and β polymorphs (7.5% w/w NaCl).

It is instructive to compare the observed eutectic point with that predicted by the equation of melting-point depression,

$$1/T = 1/T_m - (R/\Delta H_m)\ln x \quad (1)$$

where T_m is the melting point of a pure substance, ΔH_m the corresponding heat of melting, R the ideal gas constant, x the mole fraction of the solvent in the presence of an impurity (in our case mannitol in the presence of NaCl), and T the depressed melting point. Equation (1) is based on the assumption of ideal liquid mixing. Equation (1) reproduces the melting-point depression curve reported for the mannitol–sorbitol system to good precision (14). From the reported T_m and ΔH_m of mannitol (18) and the eutectic temperatures of this study, we obtained x_e (mannitol) = 0.59, which translates to a NaCl concentration of 0.41 in mole fraction and 19% w/w. These values are significantly higher than those observed (0.20 and 7.5% w/w) and indicate that NaCl depresses the melting point of mannitol more effectively than the prediction of Eq. (1) based on ideal mixing. The nonideality of the NaCl–mannitol solution is not surprising given the dissimilarity of their structures. If NaCl is treated as an un-ionized molecule, its depression of the melting point of water predicted by Eq. (1) is significantly lower than that observed (21). This discrepancy arises from the ionization of NaCl into Na^+ and Cl^- in water. It would be interesting to determine whether NaCl also ionizes in mannitol, causing more effective depression of mannitol's melting point.

NaCl vs. Other Salts

The significant miscibility between NaCl and mannitol and the effect of NaCl on the polymorphism of mannitol are unexpected, given their dissimilar structures. It was of interest to determine whether other salts exhibit similar effects. We analyzed the mixtures of mannitol with K_2SO_4, KCl, or LiCl (10% w/w salt) prepared with the same dissolution and drying method. As in the case with NaCl, mannitol existed in these mixtures as the α and β polymorphs. Some had traces of the δ polymorph. Figure 7 shows the DSC data of the mannitol–salt mixtures. Table I summarizes transition temperatures of interest. The endotherm observed in the first heating scan is attributed to the melting of the mannitol–salt eutectic. The

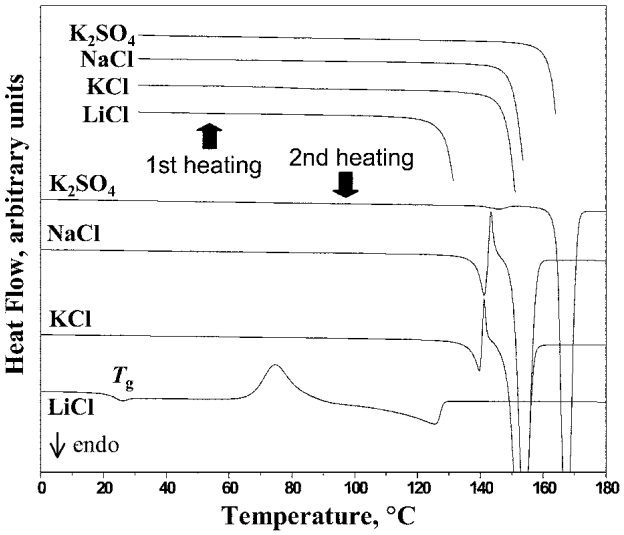

Fig. 7. Differential scanning calorimetry data of mannitol–salt mixtures (10% w/w salt, mannitol as a mixture of α and β polymorphs). The sample was scanned at 5°C/min with the following temperature program: first heating from 25°C to 190°C, cooling to −25°C, and second heating to 190°C.

Table I. Melting and Glass Transition Temperatures (T_m and T_g) of D-Mannitol and D-Mannitol–Salt Mixtures (10% w/w salt)

Salt	None	NaCl	KCl	K_2SO_4	LiCl
$T_{m\ \alpha,\beta}$, °C	165.5 (α) 165.0 (β)	150	148	165	131
$T_{m\ \delta}$, °C	155	139	136	—	—
T_g, °C	10.7	—	—	—	21

DSC features of the KCl-mannitol mixture are similar to those of the NaCl-mannitol mixture, indicating that the corresponding phase diagrams are similar. K_2SO_4 did not cause pronounced changes in the DSC behavior of mannitol, indicating no significant melt miscibility between the two components. Among the salts tested, LiCl depressed the melting point to the greatest extent and thus had the highest melt miscibility with mannitol.

When the melts were cooled to room temperature, only LiCl inhibited the crystallization of mannitol. It is remarkable that the inhibitory effect of LiCl on mannitol crystallization was greater than that of sorbitol, a stereoisomer of mannitol, at the same concentration (10% w/w) (16). On reheating, the LiCl–mannitol mixture showed a glass transition at 21°C. This T_g is higher than the T_g of mannitol (10.7°C) (16), confirming the incorporation of LiCl in amorphous mannitol. Further heating caused the crystallization of mannitol at 80°C. With the other salts, mannitol crystallized during cooling, and the subsequent reheating revealed the polymorphic outcome of crystallization in each system (Fig. 7). The DSC profile of the KCl–mannitol mixture is similar to that of the NaCl–mannitol mixture, indicating that KCl also aided the isolation of the metastable δ polymorph. With the K_2SO_4–mannitol mixture, a weak endotherm was observed at 145°C, which was absent in the first heating. This endotherm is attributed to the δ→α polymorphic transition during heating, which is sometimes detected in pure mannitol (18). Collectively, the results obtained with other salts demonstrate that the melt miscibility between mannitol and NaCl, though unexpected because of their structural dissimilarity, occurs with other salts. Although some salts are not pharmaceutically acceptable, this comparison reveals the generality of the phenomenon.

Pharmaceutical Relevance

The significant melt miscibility observed in this study between mannitol and NaCl suggests a degree of affinity between the two structurally dissimilar substances. This affinity helps explain the strong inhibitory effect of NaCl on mannitol crystallization identified by our previous study (1). It is important to note, however, that the miscibility exists only in the amorphous state. In this study, melting created the amorphous state; in frozen solutions, the residual water in the freeze concentrate is necessary to hold mannitol and NaCl together in the amorphous phase. During primary drying, when ice sublimes but the residual water remains in the freeze concentrate, NaCl is able to inhibit the crystallization of mannitol and, in this role, outperforms many other excipients (1). During secondary drying, when the residual water is removed from the freeze concentrate, crystallization of mannitol and NaCl is expected to occur. Thus, to suppress mannitol crystallization in secondary drying requires another component, which may be the API itself or other formulation ingredients (4,5,10,11) introduced for this purpose or by necessity. The accumulated understanding of how different components influence the crystallization of mannitol in different drying stages promises rational design and control of the physical state of this important excipient in lyophilized products.

CONCLUSIONS

Using DSC, HSM, Raman microscopy, and VTXRD, we determined that significant melt miscibility exists between NaCl and mannitol (7.5% w/w NaCl) and that NaCl influenced the polymorphism of mannitol. The mannitol–NaCl phase diagram is of the eutectic type with the eutectic temperature depending on the polymorph of mannitol (150°C for α and β and 139°C for δ) and the eutectic composition being 7.5% w/w NaCl. Isothermal experiments in the vicinity of the eutectic composition aided the determination of the liquidus phase boundary. The presence of NaCl did not prevent the crystallization of mannitol but influenced the polymorphic form obtained. At small sample size (<10 mg), δ was obtained; at large sample size (>100 mg), α was obtained. The dependence of the polymorphic outcome on sample size was linked to the crystallization of mannitol polymorphic modifications in two stages. The salt effect on mannitol crystallization and polymorphism is not unique to NaCl. KCl showed approximately the same eutectic melting point with mannitol as NaCl, indicating similar melt miscibility. K_2SO_4 had little effect on the crystallization of mannitol. LiCl inhibited the crystallization of mannitol during cooling and enabled the observation of its glass transition. The results are relevant to the rational design and control of the physical state of mannitol in freeze-dried products.

REFERENCES

1. C. Telang, L. Yu, and R. Suryanarayanan. Effective inhibition of mannitol crystallization in frozen solutions by sodium chloride. *Pharm. Res.* **20**:660–667 (2003).
2. E. Y. Shalaev and F. Franks. Solid-liquid diagrams in pharmaceutical lyophilization: Crystallization of solutes. In H. Levine (ed.), *Progress in Amorphous Food and Pharmaceutical Systems*, Royal Society of Chemistry, 2002, pp. 200–215.
3. M. J. Pikal. Freeze drying. In J. Swarbrick and J. C. Boylan (eds.), *Encyclopedia of Pharmaceutical Technology*, Marcel Dekker, New York, 1993, pp. 275–303.
4. A. Martini, K. Silvia, M. Crivellente, and R. Artico. Use of subambient differential scanning calorimetry to monitor the frozen state behavior of blends of excipients for freeze-drying. *PDA J. Pharm. Sci. Tech.* **51**:62–67 (1997).
5. A. I. Kim, M. J. Akers, and S. L. Nail. the physical state of mannitol after freeze-drying: effects of mannitol concentration, freezing rate, and a noncrystallizing cosolute. *J. Pharm. Sci.* **87**:931–935 (1998).
6. F. H. Cocks and W. E. Brower. Phase diagram relations in cryobiology. *Cryobiology* **11**:340–358 (1974).
7. F. W. Gayle, F. H. Cocks, and M. L. Shepard. The water–sodium chloride–sucrose phase diagram and applications in cryobiology. *J. Appl. Chem. Biotechnol.* **27**:599–607 (1977).
8. M. G. Fakes, M. V. Dali, T. A. Haby, K. R. Morris, S. A. Varia, and A. T. M. Serajuddin. Moisture sorption behavior of selected bulking agents used in lyophilized products. *PDA J. Pharm. Sci. Tech.* **54**:144–149 (2000).
9. H. R. Costantino, J. D. Andya, P. A. Nguyen, N. Dasovich, T. D. Sweeney, S. J. Shire, C. C. Hsu, and Y.-F. Maa. Effect of mannitol crystallization on the stability and aerosol performance of a spray-dried pharmaceutical protein, recombinant humanized anti-ige monoclonal antibody. *J. Pharm. Sci.* **87**:1406–1411 (1998).

10. K. Izutsu, S. Yoshioka, and T. Terao. Decreased protein-stabilizing effects of cryoprotectants due to crystallization. *Pharm. Res.* **10**:1232–1237 (1993).
11. K. Izutsu, S. Yoshioka, and T. Terao. Effect of mannitol crystallinity on the stabilization of enzymes during freeze-drying. *Chem. Pharm. Bull.* **42**:5–8 (1994).
12. R. K. Cavatur and R. Suryanarayanan. Characterization of frozen aqueous solutions by low temperature X-ray powder diffractometry. *Pharm. Res.* **15**:194–199 (1998).
13. K. Ito. Freeze drying of pharmaceuticals. Eutectic temperature and collapse temperature of solute matrix upon freeze drying of three-component systems. *Chem. Pharm. Bull.* **19**:1095–1102 (1971).
14. M. Siniti, S. Jabrane, and J. M. Letoffe. Study of the respective binary phase diagrams of sorbitol with mannitol, maltitol and water. *Thermochim. Acta* **325**:171–180 (1999).
15. H. Bauer, T. Herkert, M. Bartels, K.-A. Kovar, E. Schwarz, and P. C. Schmidt. Investigations on polymorphism of mannitol/sorbitol mixtures after spray-drying using differential scanning calorimetry, X-ray diffraction and near-infrared spectroscopy. *Pharmazeutische Industrie* **62**:231–235 (2000).
16. L. Yu, D. S. Mishra, and D. R. Rigsbee. Determination of the glass properties of D-mannitol using sorbitol as an impurity. *J. Pharm. Sci.* **87**:774–777 (1998).
17. Powder Diffraction File. (PDF-2), International Centre for Diffraction Data, Newtown Square, PA (1996).
18. A. Burger, J. O. Henck, S. Hetz, J. M. Rollinger, A. A. Weissnicht, and H. Stottner. Energy/temperature diagram and compression behavior of the polymorphs of D-mannitol. *J. Pharm. Sci* **89**:457–468 (2000).
19. B. Debord, C. Lefebvre, A. M. Guyot-Hermann, J. Hubert, R. Bouche, and J. C. Guyot. Study of different crystalline forms of mannitol: comparative behavior under compression. *Drug. Dev. Ind. Pharm.* **13**:1533–1546 (1987).
20. L. Yu. Nucleation of one polymorph by another. *J. Am. Chem. Soc.* **125**:6380–6381 (2003).
21. R. C. Weast (ed.). *CRC Handbook of Chemistry and Physics,* 50th ed., The Chemical Rubber Co., Cleveland, OH (1970).